Klebsiella pneumoniae nitrogenase: pre-steady-state absorbance changes show that redox changes occur in the MoFe protein that depend on substrate and component protein ratio; a role for P-centres in reducing dinitrogen?

David J. LOWE, Karl FISHER and Roger N. F. THORNELEY

AFRC Institute of Plant Science Research, Nitrogen Fixation Laboratory, University of Sussex, Brighton BN1 9RQ, U.K.

The pre-steady-state absorbance changes that occur during the first 0.6 s of reaction of the nitrogenase of *Klebsiella pneumoniae* can be simulated by associating redox changes with the different states of the MoFe protein described by our published kinetic model for nitrogenase [Lowe and Thorneley (1984) Biochem. J. **224**, 877–886]. When the substrate is changed, from H^+ to C_2H_2 (acetylene) or N_2, or the nitrogenase component protein ratio is altered, these pre-steady-state absorbance changes are affected in a manner that is quantitatively predicted by our model. The results, together with parallel e.p.r. studies, are interpreted as showing that the P-clusters become oxidized when the MoFe protein is in the state where bound N_2 is irreversibly committed to being reduced and is protonated to the hydrazido(2-) level.

INTRODUCTION

The molybdenum nitrogenase of *Klebsiella pneumoniae* consists of two proteins, the MoFe protein (Kp1; M_r approx. 227000) and the Fe protein (Kp2; M_r approx. 64000). It catalyses the reduction of N_2 to $2NH_3$, of aqueous $2H^+$ to H_2 and of a number of other small molecules such as C_2H_2 (acetylene) to C_2H_4 (ethylene); ATP is hydrolysed concomitantly with substrate reduction to ADP and P_i. The Fe protein contains a single [4Fe-4S] cluster. The MoFe protein contains 2 FeMoco centres of approximate composition $MoFe_{6-8}S_{4-10}$, which are probably associated with the reducible substrate-binding site. It also contains the 'P-centres', four unusual Fe-S centres that are believed to be [4Fe-4S] clusters arranged in pairs approx. 1.9 nm from each FeMoco centre. Their function is not known. Reviews on the structure and function of nitrogenase have been given by Thorneley and Lowe (1985), Orme-Johnson (1985), Burgess (1985), Smith (1990), Thorneley (1990, 1992), Smith and Eady (1992) and Lowe (1992). Recently Kim and Rees (1992) have published structural models for FeMoco and P-centres based on 0.27 nm resolution X-ray crystallographic data; in these models each FeMoco centre is a [4Fe-3S] cluster and a [1Mo-3Fe-3S] cluster bridged by non-protein ligands and the P-centres are two [4Fe-4S] clusters bridged by two thiol ligands derived from cysteine residues. *In vivo* the electron donor is a flavodoxin (Hill and Kavanagh, 1980; Nieva-Gomez et al., 1980; Thorneley and Deistung, 1988) but sodium dithionite ($Na_2S_2O_4$) has been generally used for *in vitro* kinetic studies.

We have defined a kinetic scheme that is the generally accepted basis for the understanding of the mechanism of N_2 and H^+ reduction by nitrogenase (Orme-Johnson, 1992), in a series of five papers (Thorneley and Lowe, 1983; Lowe and Thorneley, 1984a,b; Thorneley and Lowe, 1984a,b). This has subsequently been extended to include a description of the reduction of C_2H_2 by the enzyme (Lowe et al., 1990). The mechanism is described in terms of the Fe-protein (Kp2) cycle and the MoFe-protein (Kp1) cycle. In the first of these, the reversible association of reduced Kp2 with Kp1 is followed by the transfer of a single electron from Kp2 to Kp1 and the obligatory reversible dissociation of oxidized Kp2 from reduced Kp1 before the Kp2 is re-reduced by dithionite. Eight of these Fe-protein cycles are combined to produce a single MoFe-protein cycle (Scheme 1), providing the eight electron transfers required to reduce $N_2 + 8H^+$ to $2NH_3 + H_2$. Kp1 that has had n electrons transferred to it from Kp2, and has been round n Fe-protein cycles, is written as E_n. H_2 can be evolved from E_2, E_3 and E_4 (Scheme 1) independently of N_2 binding. C_2H_2 binds at E_1 and E_2 and C_2H_4 is evolved from E_3 (Lowe et al., 1990).

This paper is principally concerned with the absorbance changes that take place as the MoFe protein is reduced to the various E_n states of the MoFe-protein cycle (Scheme 1). Previous pre-steady-state stopped-flow spectrophotometric studies have been concerned with the initial electron transfer from $Kp2_{red}$ to Kp1 which is complete within 20 ms under normal conditions. Thorneley (1975) and Lowe and Thorneley (1984b) examined the reduction of the dithionite-reduced state, E_0. Fisher et al. (1991) studied the corresponding initial electron transfer when a preparation of E_1 was reduced and they concluded that this rate was independent of whether the MoFe protein was in state E_0 or E_1. We now extend this to a study of absorbance changes taking place over the first 500 ms as the Kp1 is reduced from E_0 through to E_4 and correlate them with the calculated concentrations of the various species as they change with time, substrate and component protein ratio, in order to probe the nature of the redox changes taking place in the metal clusters of Kp1.

MATERIALS AND METHODS

Purification of protein components

The *Klebsiella pneumoniae* (*oxytoca*) N.C.I.B. 12204 nitrogenase component proteins were purified and assayed as previously described (Thorneley and Lowe, 1983). Nitrogenase assays at 30 °C showed that the Kp1 and Kp2 proteins used had specific activities of 2000 and 1900 nmol of C_2H_4 produced/min per mg of protein respectively. Kp1 contained 1.3 ± 0.1 g-atom of Mo/mol of protein.

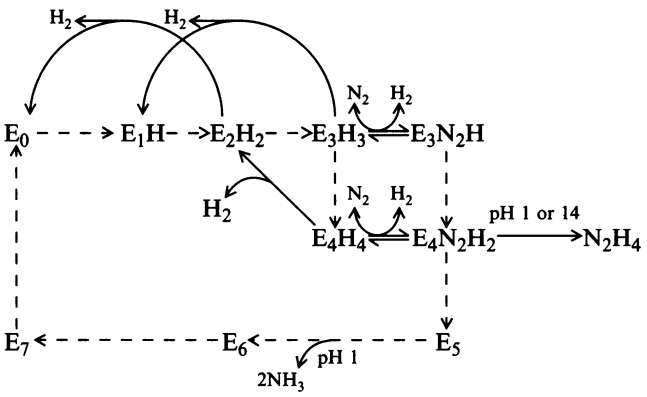

Scheme 1 The MoFe-protein cycle of nitrogenase

This scheme is a simplification of Scheme 2 of Lowe and Thorneley (1984a). Species E represent one of two independently functioning halves of the tetrameric Kp1. The subscript refers to the number of times that E has been round the electron-transfer Fe-protein cycle and therefore also indicates the number of electron equivalents by which it has been reduced relative to the resting state, E_0, which is that of Kp1 isolated in the presence of $Na_2S_2O_4$. The broken arrows linking the various E_n states each represent a single turn of the Fe-protein cycle. Side reactions at pH 1 or 14 mark where enzyme-bound intermediates give the products shown when quenched at the pHs given. The designation of structures such as E_3H_3 does not necessarily imply the existence of metal hydride intermediates or the exact level of protonation of a metal site.

Reagents and gases

All salts were purchased from BDH Chemicals; biochemicals were from Sigma Chemical Co., Poole, Dorset, U.K.

Cylinder CO and Ar were purchased from Air products, Walton-on-Thames, Surrey, U.K. C_2H_2 was prepared by the action of water on CaC_2 (calcium carbide). CO was used without further purification. Ar was passed through a heated column, containing BASF catalyst R311 granules, to a manifold that allowed alternate evacuation and Ar flushing of vials. Contaminating oxygen was removed from the C_2H_2 and CO before use by gentle shaking in a sealed 250 ml dropping funnel containing aq. 5 mM $Na_2S_2O_4$. Solutions were equilibrated with gases either by filling evacuated serum vials, with Suba-Seal closures, from the manifold (for Ar and N_2) or by flushing out Ar with an approx. threefold excess from gas-tight syringes (for C_2H_2 and CO).

Preparation of solutions

All solutions were prepared under Ar except when N_2 was to be used. The protein and ATP mixes in sealed vials were rapidly taken into a high-integrity glove box through which N_2 with an O_2 concentration below 1 p.p.m. was circulated. All solutions were taken into the glove box in 2 ml portions immediately before use to eliminate any N_2 leakage into samples over a long time period. All experiments under Ar were performed first and those under N_2 last. Samples were removed from the sealed serum vials for stopped-flow spectrophotometry using gas-tight syringes with a 7.5 cm-long wide-bore (serum O) needle attached.

Precautions were taken to exclude glove box N_2 from solutions unless the experiment was to be performed under 1 atm of N_2, when the glove-box atmosphere was allowed to come into contact with samples already prepared under N_2.

Stopped-flow spectrophotometry

Stopped-flow spectrophotometry was performed at 23 °C with a Hi-Tech SF-51 instrument (Hi-Tech Scientific, Salisbury, Wilts., U.K.) installed with a Techne-C400 thermostat (Techne Ltd., Duxford, Cambridge, U.K.) inside the anaerobic glove box operating with recirculating N_2. The poly(tetrafluoroethylene) (PTFE) tubing from the drive syringes to the glass mixing and observation cell was replaced with poly(ether ether ketone) (PEEK) tubing (Upchurch Scientific Inc., Oak Harbor, WA 98277, U.S.A.) in order to reduce gas exchange between the reactants and the N_2-saturated water circulated to thermostatically control the system. This narrow-bore tubing increased the dead-time of the apparatus to 3 ms (M. Ramjee and R. N. F. Thorneley, unpublished work). Data acquisition and curve fitting were carried out as previously described (Ashby and Thorneley, 1987). The stopped-flow machine was left in Ar-saturated buffer (25 mM Hepes, 10 mM $MgCl_2$, pH 7.4) containing 1 mM $Na_2S_2O_4$ overnight and flushed with the similar Ar-sparged buffer before filling with the first ATP and protein solutions under 1 atm of Ar.

The final concentrations after mixing were Kp1 (10 μM), Kp2 (80 μM) and ATP (9 mM) except for the data of Figure 4 where Kp2 was 10 μM. All the solutions contained $Na_2S_2O_4$ (10 mM), $MgCl_2$ (10 mM) and Hepes buffer (25 mM) at pH 7.4.

Preparation and measurement of e.p.r. samples

Equal volumes of two solutions, one with Kp1 (25 μM) and Kp2 (200 μM) and the other with ATP (18 mM), were incubated in 7.8 ml glass serum vials with Suba-seal closures in a shaking water bath at 23 °C. Both solutions also contained $Na_2S_2O_4$ (10 mM), $MgCl_2$ (10 mM) and Hepes buffer pH 7.4 (25 mM).

Before incubation in the presence of 1 atm of CO, C_2H_2 or Ar, ATP solutions were Ar sparged to remove residual N_2. Protein solutions were evacuated and Ar flushed three times. Large-bore stainless-steel needles (serum O) were used to remove 0.5 ml portions of each solution into two 1 ml syringes. These two syringes were then fitted into the inlet ports of a preflushed Perspex mixing block as previously described (Fisher et al., 1991). A 15 cm needle was attached to the exit port of the mixing block in order to deliver the mixed sample into the bottom of an e.p.r. tube which was capped with a Suba-seal closure and flushed with Ar through another needle. The 15 cm needle was used as a vent for the e.p.r. tube before attachment to the Perspex mixing block at which time the inlet Ar was turned off to avoid a high positive pressure inside the e.p.r. tube. The two 1 ml syringes were manually driven in tandem to deliver 0.2 ml from each into the e.p.r. tube which was then frozen in isopentane cooled to −140 °C; this process took approx. 5 s. Spectra showing the same features were obtained for eight different sets of samples.

E.p.r. spectra were recorded on a Bruker ER200D spectrometer at 30 K and 100 mW microwave power at 9.42 GHz using 2.0 mT field modulation at 100 kHz.

Computing

This was done on a MicroVax II computer using National Algorithm Group (NAG) subroutine D02BAF to solve the differential equations describing the reaction schemes used. Simulations were produced by multiplying the $\Delta\epsilon_{430}$ values given in the Results section by the sum of the concentrations of all species in Scheme 2 of Lowe and Thorneley (1984a) contributing to the species of Scheme 1 of the present paper; a species E_n of Scheme 1 thus includes free Kp1 at that level of reduction plus all similar species of Kp1 complexed with oxidized, reduced and inactive Kp2. The 'dead-time' of the stopped-flow apparatus

was 3 ms (M. Ramjee and R. N. F. Thorneley, unpublished work) and this was subtracted from all simulations.

RESULTS

Absorbance changes under Ar

The strategy employed was to simulate the absorbance changes occurring, after mixing Kp2 plus Kp1 with MgATP in time ranges at which different redox levels of Kp1 became populated, by using changes in absorption coefficients. The results are described by Figures 1, 2 and 3 for times of 25 ms, 150 ms and 1.0 s respectively. In each of these Figures, the simulated curve representing the main conclusions drawn from the data of the Figure is drawn as a dashed line. In order to demonstrate the logical process, the curve representing the final conclusions is shown as a solid line in Figures 1, 2 and 3. In Figures 2 and 3 the continuation of the solid curve from the previous Figure is shown as a dotted line to show the improvement obtained using the extended data.

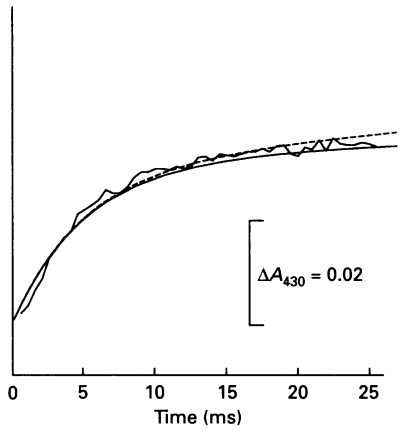

Figure 1 Absorbance changes during the first 25 ms of reaction of Kp2 with Kp1 under Ar

The concentrations for stopped-flow spectrophotometry were as described in the Materials and methods section. The solutions were equilibrated with 100% Ar before the experiment. The two smooth curves are simulations using the rate constants and assumptions of Scheme 2 of Lowe and Thorneley (1984a). Using an $\Delta\epsilon_{430}$ of 4.5 $mM^{-1}\cdot cm^{-1}$ for the oxidation of Kp2 gives the dashed curve (– – –). Using additional $\Delta\epsilon_{430}$ values, relative to E_0, of -2.2 $mM^{-1}\cdot cm^{-1}$ for E_2 and E_3, and of 4.5 $mM^{-1}\cdot cm^{-1}$ for E_4 gives the solid curve (——); these latter values are those that give the solid curve in Figure 3.

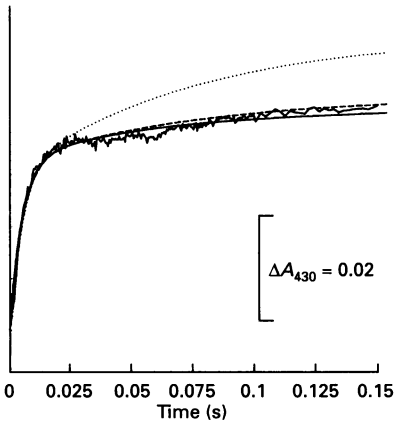

Figure 2 Absorbance changes during the first 150 ms of reaction of Kp2 with Kp1 under Ar

Conditions for the data and simulations were as in Figure 1. The simulation that gives the dotted curve (· · · ·) uses a $\Delta\epsilon_{430}$ of 4.5 $mM^{-1}\cdot cm^{-1}$ for the oxidation of Kp2. Using an additional $\Delta\epsilon_{430}$, relative to E_0, of -2.2 $mM^{-1}\cdot cm^{-1}$ for E_2 gives the dashed curve (– – –). Values, relative to E_0, of -2.2 $mM^{-1}\cdot cm^{-1}$ for E_2 and E_3 and 4.5 $mM^{-1}\cdot cm^{-1}$ for E_4 give the solid curve (——); these latter values are those that give the solid curve in Figure 3.

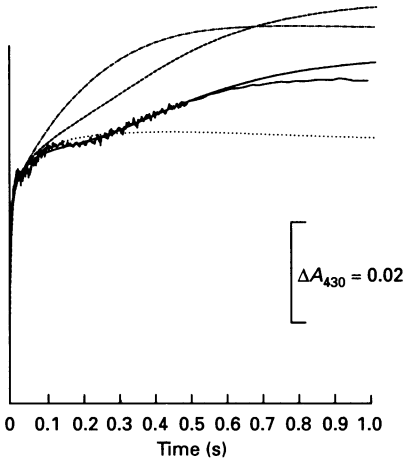

Figure 3 Absorbance changes during the first 1 s of reaction of Kp2 with Kp1 under Ar

Conditions for the data and simulations were as in Figure 1. The simulations use $\Delta\epsilon_{430}$ values of 4.5 $mM^{-1}\cdot cm^{-1}$ for the oxidation of Kp2. Using an additional $\Delta\epsilon_{430}$, relative to E_0, of -2.2 $mM^{-1}\cdot cm^{-1}$ for E_2 gives the dotted curve (· · · ·). An additional $\Delta\epsilon_{430}$, relative to E_0, of -2.2 $mM^{-1}\cdot cm^{-1}$ for E_3 and 4.5 $mM^{-1}\cdot cm^{-1}$ for E_4 gives the solid curve (——). The other two simulations use the same parameters as the solid line except for the absorbance coefficients of E_3 and E_4 relative to E_0; for the short dashed line (– – –) these relative $\Delta\epsilon_{430}$ values are 0.0 and 4.5 $mM^{-1}\cdot cm^{-1}$ respectively, and for the dot/dashed line (–·–·–) they are 4.5 and 4.5 $mM^{-1}\cdot cm^{-1}$ respectively.

Figure 1 shows the initial increase in absorbance occurring during the first 25 ms when Kp2 is oxidized by Kp1 with [Kp2]/[Kp1] = 8:1; the data are similar to those of Figure 1(a) of Thorneley (1975) where [Kp2]/[Kp1] was 1:1. The dashed line through the experimental data is a simulation using the complete Scheme 2 and rate constants in Table 1 of Lowe and Thorneley (1984a) with a $\Delta\epsilon_{430}$ of 4.5 $mM^{-1}\cdot cm^{-1}$ (Ashby and Thorneley, 1987) for the oxidation of Kp2; the almost coincident solid line uses the final conditions that include the contributions from Kp1 discussed below. The similarity of the two simulations shows that the curve is dominated by the Kp2 oxidation in this time range, although the excellence of the fit is perhaps not surprising since the simulated curve is dominated by the rate of electron transfer from Kp2 to Kp1 within the protein complex; this was measured from similar data by Thorneley (1975). The correspondence of the amplitudes of the data and the simulation, however, shows that the reduction of Kp1 from E_0 to E_1 (Scheme 1) does not involve any significant absorbance changes at this wavelength ($\Delta\epsilon_{430} < 0.5$ $mM^{-1}\cdot cm^{-1}$). No other redox levels of Kp1 (beyond E_1) are significantly populated (< 6% at 25 ms) during this time period. We have confirmed that conversion of Kp1 from state E_0 into state E_1 does not involve a significant absorbance change (< 0.5% over the range 400–750 nm, results not shown) by using a limited concentration of Kp2 (0.2 μM) to produce a steady-state concentration of Kp1 (20 μM) in 50% state E_0 and 50% state E_1 as described by Fisher et al. (1991). Difference spectra were recorded on a Perkin–Elmer Lambda 5 spectrophotometer at 23 °C at intervals up to 45 min after initiation

of the reaction by the addition of ATP (5 mM). We have previously shown that approx. 12 min is required to reach a steady state with Kp1 50% reduced to state E_1 (Fisher et al., 1991).

In Figure 2 we show the effect of observing up to 150 ms. The dotted line shows the continuation of the dashed curve from Figure 1; it is clearly an inadequate simulation of the experimental curve in this time range. At 50 ms, when 16% of the Kp1 is in state E_2, the deviation is marked and it continues to increase up to 150 ms when 33% of the Kp1 is in state E_2. The dashed line, however, gives a good simulation by assuming that the transfer of the second electron from Kp2 to Kp1 (to give E_2) results in a $\Delta\epsilon_{430}$ of $-2.2\ mM^{-1}\cdot cm^{-1}$. For Fe-S centres, a decrease in absorbance is normally assumed to be a consequence of the reduction of the cluster; we therefore associate such a reduction with the transfer of the second electron to Kp1. Note that at 50 ms, < 1% of the Kp1 is at levels other than E_0, E_1 and E_2. The final simulation is again shown by the solid line.

Finally Figure 3 shows the time course of absorbance changes occurring up to 1 s. The dotted line is the continuation of the dashed line simulation of Figure 2 and is again inadequate. The solid line simulation, which follows the major changes in slope of the experimental curve up to 0.6 s, assumes that there is no change in absorbance as E_2 is reduced to E_3 and that there is an increase in absorbance corresponding to a $\Delta\epsilon_{430}$ of $4.5\ mM^{-1}\cdot cm^{-1}$ as E_3 is reduced to E_4.

For times up to 600 ms, all deviations between the simulation and the experimental curve are less than 0.002 absorbance unit and correspond to $\Delta\epsilon_{430}$ values of less than $0.5\ mM^{-1}\cdot cm^{-1}$; we regard these as not important at this level of resolution. Nevertheless there is a small but reproducible deviation that can be seen between 30 and 200 ms such that the simulation is at the lower edge of the experimental noise below about 100 ms and at the upper edge at the longer times. This oscillation is less than 20% of the deviations that we have used to derive our absorption coefficients and cannot be simulated using the procedures in this paper since no intermediates of Scheme 1 are changing concentration in a manner consistent with it. What is therefore clear is that these small absorbance changes occur, not as a result of reactions involving component protein association or dissociation or intermolecular electron transfers, but as a result of intramolecular reactions at the E_2 level of reduction of MoFe protein; these reactions could be the transfer of electrons between clusters within the MoFe protein or from clusters to bound protons to give bound hydrides.

Figure 3 shows two additional simulations which demonstrate the effects of other assumptions. The short dashed line shows the simulation obtained if E_3 is assumed to have the same absorbance as E_1 and E_0, and the dot/dashed line shows the curve when E_3 has the same absorbance as E_4. The solid line is clearly the best fit to the data. The increase in absorbance on reduction of Kp1 from E_3 to E_4 can be assumed to be due to the oxidation of an Fe-S cluster. The overall changes in absorption coefficient associated with Kp1 are summarized in Table 1.

The deviations between the experimental and simulated curves at times longer than 0.6 s are due to the onset of inhibition of nitrogenase by ADP, since ATP was rapidly hydrolysed at the high concentrations of proteins used, and are the start of a slow decrease in absorbance that takes place over about 30 s as this inhibition takes effect. The apparent K_{IADP} and K_{DATP} have not been measured under these conditions, nevertheless the value at a [Kp2]/[Kp1] of 1:1 (20 μM and 0.4 mM respectively; Thorneley and Cornish-Bowden, 1977), together with the calculated quantity of ATP hydrolysed if 2 ATPs are hydrolysed for each electron transferred, suggest that the enzyme activity could be 25% inhibited at 1 s; the actual inhibition will be less than this since more free $Kp2_{red}$ will be available at the higher [Kp2]/[Kp1] ratio used in our experiments.

Table 1 Summary of absorption coefficient changes associated with MoFe protein (Kp1) during the pre-steady-state phase of substrate reduction

Reaction	$\Delta\epsilon_{430}$ ($mM^{-1}\cdot cm^{-1}$)	Comment
$E_0 \rightarrow E_1$	< 0.5	FeMoco reduced to e.p.r.-silent state
$E_1 \rightarrow E_2$	−2.2	Negative $\Delta\epsilon_{430}$ assumed to be due to P-cluster or FeMoco reduction
$E_2 \rightarrow E_3$	< 0.5	
$E_3 \rightarrow E_4$	+6.7	P-cluster oxidation indicated by e.p.r. under Ar and N_2, but not C_2H_2 when E_4 state is not achieved

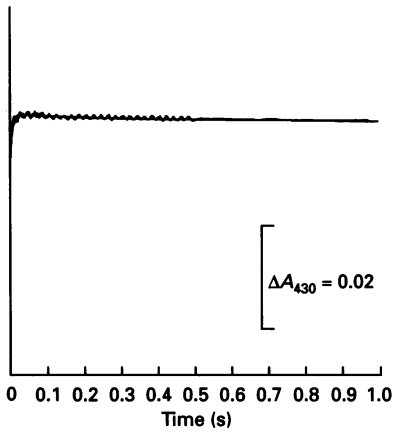

Figure 4 Absorbance changes during the first 1 s of reaction of Kp2 with Kp1 under Ar when [Kp2]/[Kp1] is 1:1

Conditions for the data were as in Figure 1 except that [Kp2] was 10 μM. The simulation uses the same scheme and relative absorption coefficients as the solid line in Figure 3.

Effect of changing the component protein ratio

In the above section we have used relative absorption coefficients for different Kp1 intermediates in Scheme 1 to explain the time course of ϵ_{450} at a [Kp2]/[Kp1] of 8:1. The validity of this model can be tested by varying the proportions of these intermediates present and comparing the experimental time course with a simulation using these same assumptions. It is possible to vary the proportion of Kp1 that is at E_4 in the steady state by varying the component protein ratio. An example of this is shown by the data of Figure 4 which were obtained with a [Kp2]/[Kp1] of 1:1 in the presence of Ar and which can be compared with the data of Figure 3 at 8:1. The solid line through the data is a simulation using exactly the same parameters as for the solid line in Figure 3, but using the different Kp2 concentration, and shows that the effect of varying [Kp2]/[Kp1] can be simulated quantitatively by the Scheme. This is principally because at, for example 0.5 s, under the conditions of Figure 4 and Figure 3, the population of species E_4 are 23% and < 0.01% of the total Kp1 respectively. Note that at times longer than 0.6 s, the simulation of Figure 4 is a closer fit to the data than that of Figure 3; this is because the rate of hydrolysis of ATP is less at the lower component ratio.

Absorbance changes under C_2H_2

In the light of the assumptions required to simulate accurately the absorbance changes that occurred under Ar, it was of interest to examine the effect of adding C_2H_2 since, according to Lowe et al. (1990), Kp1 with C_2H_2 bound cannot be reduced below the E_3 level (Scheme 1). Figure 5(a) shows the result of such an experiment at a [Kp2]/[Kp1] of 8:1 and demonstrates that the oxidation that occurred as E_3 was reduced to E_4 in the absence of C_2H_2 did not occur in its presence. The solid line is a good simulation of the experimental data whereas the dashed line, which shows the final simulation of Figure 3 to demonstrate the effect of adding C_2H_2 more clearly, is not. The solid line uses the same parameters as the final simulation of Figure 3 but conversion of E_3 into E_4 does not occur in the presence of C_2H_2 since the C_2H_2-bound species that Lowe et al. (1990) added to Scheme 2 of Lowe and Thorneley (1984a) become populated instead; the simulation assumes that binding of C_2H_2 to a species has no effect on its absorption coefficient except that C_2H_2 bound to E_3 is reduced to C_2H_4 in the protein complex so that the absorption coefficient of this species is the same as E_1. Note that the oscillation in Figure 3 that the simulation does not predict is not observable under C_2H_2 when H_2 is not evolved; this would be consistent with the above suggestion that it is related to the transfer of electrons from a metal cluster to bound protons.

Absorbance changes occurring under N_2

Figure 5(b) shows the absorbance changes occurring over the first second of reaction time in the presence of N_2. These are very similar to those under Ar alone and can be simulated by the scheme with the final parameters used in Figure 3, as shown by the solid line. Note, however, that species E_5 to E_7 of Scheme 1 become populated in the presence of N_2.

Absorbance changes occurring under CO

The first second of the time course in the presence of the inhibitor CO is given in Figure 5(c). No kinetic model exists for the redox states of Kp1 under CO and so no simulation is shown. However, the variation of absorbance with time indicates that in this case an oxidation occurs following state E_3 which is intermediate between those under C_2H_2 and Ar or N_2.

Effect of different gas phases on e.p.r. signals during turnover

Figure 6 shows the e.p.r. signals in the region $g = 12$ to $g = 3$ obtained from nitrogenase turning over in the presence of Ar, N_2, C_2H_2 and CO. Since the e.p.r. features being examined were of very low intensity, Figure 6 uses spectra that were accumulated for a total of 5.9 h. All spectra exhibited weak features at $g = 4.3$ and $g = 3.7$ given by the FeMoco centres in state E_0, as well as a broad feature between $g = 6$ and $g = 4$ which is probably from reduced Kp2 (Hagen et al., 1985). Of greater interest in the context of the present work are the sharp signals at $g = 5.4$ and $g = 5.7$ seen in the presence of Ar (Figure 6d) and N_2 (Figure 6b), but not in the presence of C_2H_2 (Figure 6a) or CO (Figure 6c). These signals were first described by Lowe et al. (1978) who showed by ^{57}Fe substitution that they were associated with Fe atoms in the MoFe protein. They are similar to S = 7/2 spin state signals observed from P-centres oxidized by solid thionine (Hagen et al., 1987) or by ferricyanide (D. J. Lowe, C. A. Gormal and B. E. Smith, unpublished work). The feature at $g = 10.4$ that

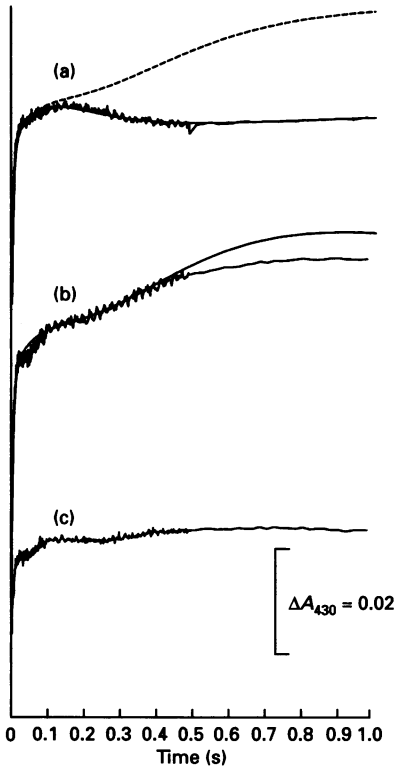

Figure 5 Absorbance changes during the first 1 s of reaction of Kp2 with Kp1 under C_2H_2, N_2 and CO

Conditions for the data and simulations were as in Figure 1 except that for (**a**) 100% C_2H_2 was equilibrated with the solutions and included in the simulation so that the additional species present under C_2H_2 described by Lowe et al. (1990) become populated, (**b**) 100% N_2 was equilibrated with the solutions and included in the simulation so that species E_5, E_6 and E_7 (Scheme 1) become populated and (**c**) 100% CO was equilibrated with the solutions but no simulation is given. For the simulations, the $\Delta\epsilon_{430}$ values used, relative to E_0, were the same as for the solid curve in Figure 3 with the addition that E_3 with C_2H_2 bound had a $\Delta\epsilon_{430}$ of 0.0 $mM^{-1} \cdot cm^{-1}$ relative to E_0.

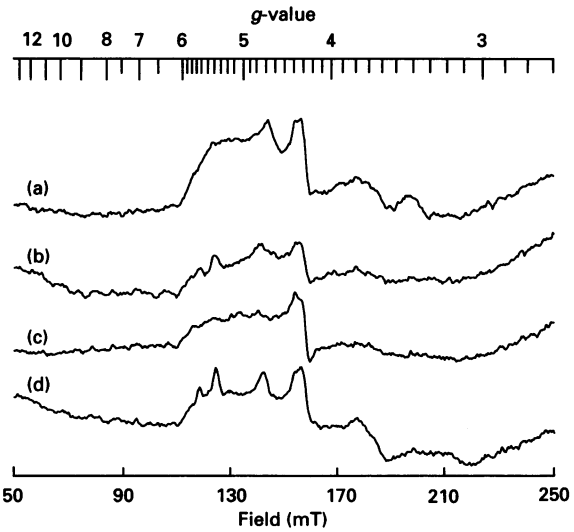

Figure 6 E.p.r. spectra from nitrogenase turning over in the presence of various gasses

Conditions were as given in the Materials and methods section. The samples were prepared in the presence of an atmosphere of 100% (**a**) C_2H_2, (**b**) N_2, (**c**) CO and (**d**) Ar.

should be associated with the $g = 5.4$ and 5.7 signal, according to the assignment of Hagen et al. (1987), could not be observed in our samples of active enzyme at a variety of microwave powers and temperatures. As our signals were very weak we were unable to measure the dependence of their intensity on temperature. Since such signals have been observed from P-centres, but not from FeMoco, we suggest that they are given by oxidized P-centres and that they can be assigned to two different types of $\pm 3/2$ manifolds of $S = 7/2$ spin systems.

DISCUSSION

The analysis that we have undertaken has shown that the metal cluster centres of a nitrogenase MoFe protein undergo redox changes as electrons are transferred from the Fe protein. These changes do not, however, correspond to the number of electrons that have been transferred and it is interesting to speculate on which centres accept the electrons.

We have shown that the initial reduction, generating E_1 (Scheme 1), results in no significant change in absorbance, although the e.p.r. signal of bound FeMoco is bleached and the change in Mössbauer spectrum is consistent with a reduction of FeMoco (Smith and Lang, 1974; Münck et al., 1975). Hence the orbitals containing the unpaired electron(s) are not associated with any optical transitions contributing significantly to the ϵ_{430}.

The second electron transfer giving E_2, however, results in an absorbance change corresponding to a reduction of a metal cluster. This suggests that even though E_2 is capable of releasing H_2, and also gives H_2 on quenching in acid (Lowe and Thorneley, 1984a), the electron density resides on the cluster and not on bound dihydrogen. No further optical change is observed when E_3 is formed.

The formation of E_4 is the most interesting, in that it is the species that must be reached before MoFe protein with N_2 bound becomes irreversibly committed to reducing the N_2 (Thorneley and Lowe, 1984a). We have now shown by optical absorbance changes that its reductive formation is associated with an oxidation of a cluster within the MoFe protein, and furthermore by e.p.r. that the centres oxidized are likely to be the P-clusters of hitherto unknown function. We suggest therefore that when E_4 is reached, a transfer of electron density from the P-centres on to FeMoco is triggered and that this generates an increased reducing power. Electron transfers between these clusters are possible since the shortest distance between metal sites on FeMoco and the associated P-cluster pair is about 1.4 nm (Kim and Rees, 1992). Thorneley and Lowe (1984a) explained that it was necessary to introduce an irreversible step at E_4, after N_2 binding, in order to derive the correct form for the dependence of the K_m for N_2 on [Kp2]/[Kp1]; they suggested that this step was a protonation of bound N_2 to the hydrazido(2-) level. Thorneley et al. (1978) have identified an intermediate during N_2 reduction that gives rise to hydrazine on quenching in acid or alkali and proposed that this was bound N_2 reduced to the hydrazido(2-) level (species $E_4N_2H_4$ in Scheme 1). Thorneley and Lowe (1984a) subsequently showed that this intermediate is the dominant species of E_4 present when nitrogenase is reducing N_2. We now propose that protonation to give this intermediate occurs because of the oxidation of P-centres with a parallel increase of electron density on N_2 bound to FeMoco and that this is the crucial step that gives nitrogenase the ability to reduce dinitrogen.

We thank Dr. H. Haaker, Dr. R. L. Richards and Professor B. E. Smith for helpful discussions.

REFERENCES

Ashby, G. A. and Thorneley, R. N. F. (1987) Biochem. J. **246**, 455–465
Burgess, B. K. (1985) in Metal Ions in Biology Series; vol. 7: Molybdenum Enzymes (Spiro, T. G., ed.), pp. 161–219, Wiley Interscience, New York
Fisher, K., Lowe, D. J. and Thorneley, R. N. F. (1991) Biochem. J. **279**, 81–85
Hagen, W. R., Eady, R. R., Dunham, W. R. and Haaker, H. (1985) FEBS Lett. **189**, 250–254
Hagen, W. R., Wassink, H., Eady, R. R., Smith, B. E. and Haaker, H. (1987) Eur. J. Biochem. **169**, 457–465
Hill, S. and Kavanagh, E. P. (1980) J. Bacteriol. **141**, 470–475
Kim, J. and Rees, D. C. (1992) Science **257**, 1677–1682
Lowe, D J. (1992) in Electron and Proton Transfer in Chemistry and Biology (Müller, A., Ratajczak, H., Junge, W. and Diemann, E., eds.), pp. 149–165, Elsevier, Amsterdam
Lowe, D. J. and Thorneley, R. N. F. (1984a) Biochem. J. **224**, 877–886
Lowe, D. J. and Thorneley, R. N. F. (1984b) Biochem. J. **224**, 895–901
Lowe, D. J., Eady, R. R. and Thorneley, R. N. F. (1978) Biochem. J. **173**, 277–290
Lowe, D. J., Fisher, K. and Thorneley, R. N. F. (1990) Biochem. J. **272**, 621–625
Münck, E., Rhodes, H., Orme-Johnson, W. H., Davis, L. C., Brill, W. J. and Shah, V. K. (1975) Biochim. Biophys. Acta **400**, 32–53
Nieva-Gomez, D., Roberts, G. P., Klevickis, S. and Brill, W. J. (1980) Proc. Natl. Acad. Sci. U.S.A. **77**, 2555–2558
Orme-Johnson, W. H. (1985) Annu. Rev. Biophys. Biophys. Chem. **14**, 419–459
Orme-Johnson, W. H. (1992) Science **257**, 1639–1640 and references therein
Smith, B. E. (1990) in Nitrogen Fixation: Achievements and Objectives (Gresshof, P. M., Roth, L. E., Stacey, G. and Newton, W. E., eds.), pp. 3–13, Chapman and Hall, New York and London
Smith, B. E. and Eady, R. R. (1992) Eur. J. Biochem. **205**, 1–15
Smith, B. E. and Lang, G. (1974) Biochem. J. **137**, 169–180
Thorneley, R. N. F. (1975) Biochem. J. **145**, 391–396
Thorneley, R. N. F. (1990) in Nitrogen Fixation: Achievements and Objectives (Gresshof, P. M., Roth, L. E., Stacey, G. and Newton, W. E., eds.), pp. 103–109, Chapman and Hall, New York and London
Thorneley, R. N. F. (1992) Philos. Trans. R. Soc. London Ser. B **336**, 73–82
Thorneley, R. N. F. and Cornish-Bowden, A. (1977) Biochem. J. **167**, 457–461
Thorneley, R. N. F. and Deistung, J. (1988) Biochem. J. **253**, 587–595
Thorneley, R. N. F. and Lowe, D. J. (1983) Biochem. J. **215**, 393–403
Thorneley, R. N. F. and Lowe, D. J. (1984a) Biochem. J. **224**, 887–894
Thorneley, R. N. F. and Lowe, D. J. (1984b) Biochem. J. **224**, 903–909
Thorneley, R. N. F. and Lowe, D. J. (1985) in Metal Ions in Biology Series; vol. 7: Molybdenum Enzymes (Spiro, T. G., ed.), pp. 117–159, Wiley Interscience, New York
Thorneley, R. N. F., Eady, R. R. and Lowe, D. J. (1978) Nature (London) **272**, 557–558

Received 18 June 1992/9 November 1992; accepted 27 November 1992